Thiazolidinedione Treatment Decreases Oxidative Stress in Spontaneously Hypertensive Heart Failure Rats Through Attenuation of Inducible Nitric Oxide Synthase–Mediated Lipid Radical Formation

Maria B. Kadiiska,[1] Marcelo G. Bonini,[2] Christine Ruggiero,[3] Ellen Cleland,[3] Shawna Wicks,[3] and Krisztian Stadler[3]

The current study was designed to test the hypothesis that inducible nitric oxide synthase (iNOS)-mediated lipid free radical overproduction exists in an insulin-resistant rat model and that reducing the accumulation of toxic metabolites is associated with improved insulin signaling and metabolic response. Lipid radical formation was detected by electron paramagnetic resonance spectroscopy with in vivo spin trapping in an obese rat model, with or without thiazolidinedione treatment. Lipid radical formation was accompanied by accumulation of toxic end products in the liver, such as 4-hydroxynonenal and nitrotyrosine, and was inhibited by the administration of the selective iNOS inhibitor 1400 W. The model showed impaired phosphorylation of the insulin signaling pathway. Ten-day rosiglitazone injection not only improved the response to an oral glucose tolerance test and corrected insulin signaling but also decreased iNOS levels. Similar to the results with specific iNOS inhibition, thiazolidinedione dramatically decreased lipid radical formation. We demonstrate a novel mechanism where a thiazolidinedione treatment can reduce oxidative stress in this model through reducing iNOS-derived lipid radical formation. Our results suggest that hepatic iNOS expression may underlie the accumulation of lipid end products and that reducing the accumulation of toxic lipid metabolites contributes to a better redox status in insulin-sensitive tissues. ***Diabetes*** **61:586–596, 2012**

Obesity and type 2 diabetes are associated with insulin resistance and linked to increased risk for several complications, such as cardiovascular diseases (1,2) or hypertension (3), that are leading causes of death for these patients. There is a common understanding that the insulin signaling phosphorylation cascade is impaired in insulin resistance in the peripheral tissues (4). Evidence indicates that any impairment related to insulin signaling proteins, including the phosphorylation of Ser instead of Tyr on the insulin receptor (IR) and IR substrates (IRSs) (5,6), contributes to the development of insulin resistance. The molecular mechanisms underlying insulin resistance have been intensely investigated over the past years, often focusing on the possible contribution of increased oxidative stress, its toxic end products, and the accompanying low-grade inflammation (7–10).

Insulin resistance and type 2 diabetes are frequently associated with chronic low-grade inflammation. Inducible nitric oxide synthase (iNOS) is often a mediator in inflammatory processes and insulin resistance (11–15). The enzyme is expressed in insulin-sensitive organs in both rodents and humans. Its expression is upregulated by many inducers of insulin resistance, such as hyperglycemia (16,17), free fatty acids (11), and cytokines (18,19). Studies include high-fat diet–fed mice, Zucker rats, various animal models, and diabetic patients (20–24). Our work in a streptozotocin-induced diabetes model demonstrated a significant role for dysfunctional iNOS. Oxidant stress and inflammation may lead to the generation of peroxynitrite and its decomposition products, such as hydroxyl radicals, which initiate the self-propelling process of lipid peroxidation (25).

There is increasing evidence that accumulation of toxic lipid metabolite end products from lipid peroxidation processes may compromise insulin signaling (26). Although the underlying mechanisms are not yet well understood, this process is associated with the onset and development of insulin resistance in those tissues that are not designed for fat storage, such as skeletal muscle and liver. Reactive species and free radicals can stimulate reactions with polyunsaturated fatty acids, leading to lipid hydroperoxides, which are unstable and decompose to various lipid peroxidation end products, including 4-hydroxynonenal (4-HNE) (27). 4-HNE is a toxic aldehyde that can accumulate as a result of increased oxidative stress and lipid peroxidation (28,29). 4-HNE is able to covalently bind and modify proteins (30,31). Furthermore, various lipid peroxides and lipid peroxyl radicals can initiate further reactions and, according to novel studies, mediate dimerization or nitration of proteins in certain conditions (32,33). Because Tyr phosphorylation is crucial for intact insulin signaling, modification of Tyr residues on these proteins can be deleterious to their function.

In this study, we investigated an obese model, the spontaneously hypertensive heart failure (SHHF) rat. We tested the hypothesis that lipid free radical generation contributes to redox imbalance and that a diabetic treatment can attenuate this mechanism. With electron paramagnetic resonance (EPR) spectroscopy and immunological methods, we demonstrate increased lipid radical formation and

From the [1]Laboratory of Pharmacology and Chemistry, National Institute of Environmental Health Sciences, National Institutes of Health, Research Triangle Park, North Carolina; the [2]Section of Cardiology, Department of Pharmacology, University of Illinois, Chicago, Illinois; and the [3]Oxidative Stress and Disease Laboratory, Gene-Nutrient Interaction Laboratory, Pennington Biomedical Research Center, Louisiana State University, Baton Rouge, Louisiana.

Corresponding author: Krisztian Stadler, krisztian.stadler@pbrc.edu.

Received 8 August 2011 and accepted 6 December 2011.

DOI: 10.2337/db11-1091

This article contains Supplementary Data online at http://diabetes.diabetesjournals.org/lookup/suppl/doi:10.2337/db11-1091/-/DC1.

M.B.K. and M.G.B. contributed equally to this study.

the accumulation of the harmful end products 4-HNE and 3-nitrotyrosine in insulin-sensitive tissues of these obese rats. The lipid radical formation was inhibitable with the iNOS inhibitor *N*-(3-aminomethyl)benzylacetamidine (1400 W), as well as with a 10-day thiazolidinedione treatment. Thiazolidinedione treatment reduced not only lipid radical formation but also hepatic iNOS protein levels, suggesting a potential mechanistic relation between these processes. Decreased oxidative stress was associated with better metabolic response and insulin signaling. Our study shows that obesity, increased lipid load, and enhanced lipid peroxidation work synergistically to increase free radical generation, which can be attenuated partially through inhibition of iNOS.

RESEARCH DESIGN AND METHODS

α-(4-Pyridyl-1-oxide)-*N*-*t*-butylnitrone (POBN) and rosiglitazone were obtained from Alexis Biochemicals (San Diego, CA). The 1400 W was from Calbiochem-Novabiochem (La Jolla, CA). Other materials were all obtained from Sigma-Aldrich (St. Louis, MO).

Ten-week-old Wistar-Kyoto (WKY) male rats (Charles River Laboratories) were used in all experiments as controls; age-matched male spontaneously hypertensive heart failure (SHHF) rats were used as obese animals. Rats were housed in a room with air conditioning and a 12/12 h light/dark cycle, were fed a standard rat chow (NIH open formula; Zeigler Brothers, Gardners, PA), and had access to water ad libitum. All studies were approved by the institutional review boards at the National Institute of Environmental Health Sciences and the Pennington Biomedical Research Center and adhered to National Institutes of Health guidelines for the care and handling of experimental animals.

Body composition. Body composition was characterized by a Bruker Mini-Scope NMR (Bruker, Billerica, MA) at the Pennington Biomedical Research Center. WKY and SHHF rats were placed in a plastic tube and their lean mass, fat mass, and free fluid amounts were compared.

In vivo studies. For the EPR experiments, POBN was dissolved in saline and administered at 1 g/kg body wt i.p. and bile cannulation was performed. Bile samples (~300 μL) were collected every 30 min for 2.5 h into plastic Eppendorf tubes containing a 50-μL solution of bathocuproine disulfonic acid and 2,2'-dipyridyl (30 mmol/L, respectively, to prevent ex vivo free radical production). Samples were frozen in dry ice immediately after collection and stored at −80°C until the EPR measurements.

In the inhibitor studies, WKY or SHHF rats received the iNOS inhibitor 1400 W (15 mg/kg i.p.) 1 h before bile cannulation and spin trapping. Each group contained at least six animals. A different group of animals received L-arginine (100 mg/kg i.p.) 30 min before spin trapping experiments. The rosiglitazone-treated group received rosiglitazone for 10 days (4 mg/kg/day i.p.). Another group received the cell permeable free radical scavenger 4-hydroxy-2,2,6,6-tetramethylpiperidine-*N*-oxyl (TEMPOL) for 10 days (30 mg/kg/day i.p). Control groups received vehicle only.

For the various experiments with the insulin signaling pathway proteins, liver and skeletal muscle samples were taken from WKY and SHHF rats after insulin stimuli. Anesthetized animals received human insulin (50 IU/kg) via the portal vein; liver and skeletal muscle samples were taken 30 and 90 s, respectively, after the stimuli and frozen immediately in liquid nitrogen.

For oral glucose tolerance test (OGTT), WKY and SHHF rats received 300 mg/100 g body wt glucose in solution via oral gavage. Blood glucose levels were tested at 0, 30, 60, 90, and 120 min after OGTT with a OneTouch Mini apparatus.

EPR studies. All EPR spectra were recorded at room temperature in a quartz flat cell on a Bruker EMX EPR spectrometer equipped with a super high-Q cavity. Spectra were recorded using an IBM-compatible computer interfaced with the spectrometer with the following instrument settings and conditions: 20.2 mW microwave power, 100 kHz modulation frequency, 1 G modulation amplitude, 1,300 ms time constant, 655 ms conversion time, and a single scan of 80 G. Bile samples were treated with ascorbate oxidase strips to reduce the interfering background signal of ascorbate radical that is abundant in bile.

Immunoprecipitation. For immunoprecipitation studies, polyclonal IR-β antibody was obtained from Santa Cruz Biotechnology (San Diego, CA). Polyclonal IRS-1 antibody from Millipore was used to immunoprecipitate IRS-1. Polyclonal rabbit Akt as well as p-Ser473-Akt antibodies were purchased from Cell Signaling Technology (Danvers, MA) to detect or immunoprecipitate these proteins. Phospho-IR-β (Tyr1162), phosphatidylinositol 3-kinase (PI3K)-p85 subunit, and pIRS (Tyr989) antibodies were purchased from Santa Cruz Biotechnology. Liver and skeletal muscle tissue samples were homogenized with a Polytron homogenizer in lysis buffer containing a mixture of protease and phosphatase inhibitors, 2% Triton X-100, 300 mmol/L NaCl, 20 mmol/L Tris, 2 mmol/L EDTA, and 1% Nonidet P-40. Samples were centrifuged at 10,000 rpm for 5 min at 4°C. Protein concentrations were quantitated with a BCA protein assay kit (Pierce). Supernatants containing 1,500 μg protein were incubated with various polyclonal antibodies according to the manufacturer's recommendation (typically 4 μg antibody) overnight in 4°C. These samples were then incubated with 40–100 μL Protein A Plus agarose beads (Pierce) for 2 h at 4°C. The beads were prewashed three times with cold PBS before use. Complexes were centrifuged at 3,000 rpm for 1 min between exhaustive washing steps with cold lysis buffer (at least five washes). For Western blot analysis, beads containing the immunoprecipitated protein were incubated in 50 μL elution buffer for 10 min and then 30 μL SDS sample buffer was added. In some experiments, eluates were boiled for 10 min. Supernatants were separated on reducing NuPAGE 4–12% Bis-Tris gels (Invitrogen) and transferred to a nitrocellulose membrane.

Western blotting. Liver or skeletal muscle homogenate supernatants containing equal amounts of protein were reduced similarly to the previous procedure, and 20–40 μg protein per lane was loaded for electrophoresis and transferred as described above. For nuclear fractionation, liver samples were homogenized in a buffer containing 0.32 mol/L sucrose, 20 mmol/L Tris-HCl (pH 7.4), 2 mmol/L EDTA, 1 mmol/L dithiothreitol, and protease inhibitor cocktail at 4°C. The homogenates were centrifuged (1,000*g*, 25 min, 4°C) and the pellets were washed once with this buffer (1,000*g*, 10 min, 4°C), suspended in Triton buffer (1% Triton X-100, 20 mmol/L Tris-HCl [pH 7.4], 150 mmol/L NaCl, 200 mmol/L EDTA, plus protease inhibitor cocktail), kept on ice for 30 min, and centrifuged (15,000*g*, 30 min, 4°C) to obtain the nuclear fraction.

After blocking (1% BSA in 0.1 mol/L PBS, pH = 7.4), the membrane was probed with the corresponding antibody against the protein of interest in the immunoprecipitation studies (IR-β, pIR-β, IRS-1, p85, pIRS-1, Akt, or p-Ser473-Akt). In the case of whole homogenates, monoclonal anti-iNOS antibody (Sigma-Aldrich), polyclonal IRS-1 primary (Millipore), goat primary anti–peroxisome proliferator–activated receptor (PPAR)-γ coactivator 1-α (anti–PGC1-α; Novus Biologicals), rabbit primary anti-PEPCK (Cell Signaling), or anti-G6Pase (Santa Cruz Biotechnology) were used, followed by the appropriate secondary antibody conjugated with horseradish peroxidase (1:10,000) and development by enhanced chemiluminescent substrate (Pierce). Western blot band intensities were quantified using the ImageJ program (download available at http://rsb.info.nih.gov/ij/).

Confocal microscopy. For confocal studies, liver and skeletal muscle samples from WKY and SHHF rats were fixed in 4% buffered formaldehyde for 24 h then placed into 30% sucrose for 24 h. Tissues were then embedded into optimal cutting temperature media, sliced on a cryocut microtome into 30-μm sections, and mounted on frosted glass slides. Samples were permeabilized with 0.1% Surfact-Amps-X-100 for 30 min. After blocking with 1% BSA in PBS for 30 min, staining of 4-HNE was performed using polyclonal anti–HNE-adduct primary antibody (Axxora, San Diego, CA) (1:500) and an Alexa Fluor 488 anti-mouse fluorescent secondary antibody (1:1,000). Staining for nitrotyrosine was made using Abcam anti-nitrotyrosine primary (1:500) and Alexa Fluor 568 secondary (1:1,000) antibodies. Secondary controls were done by omitting the primary antibody but applying the secondary antibody. Sections were observed under an LSM510 confocal laser microscope (Zeiss).

Tissue nitrite levels. Liver and skeletal muscle nitrite levels were determined with the Griess method using a nitrite measurement kit obtained from Invitrogen.

Statistical analysis. Data are expressed as mean ± SD. Statistical significance between groups was determined by ANOVA and Student *t* test as appropriate. $P < 0.05$ was considered to be statistically significant.

RESULTS

Body composition and impaired glucose tolerance in SHHF rats. Compared with their age-matched controls, SHHF rats showed increase in their fat mass and free fluid content (Fig. 1*A*–*C*). WKY and obese SHHF rats were subjected to an oral glucose challenge after overnight fasting to confirm the presence of impaired oral glucose tolerance. As shown in Fig. 1*D*, SHHF rats were unable to recover their blood glucose levels in time compared with age-matched WKY. This result confirms that SHHF rats are glucose intolerant, a characteristic feature of metabolic syndrome.

Increased lipid radical formation in SHHF rats with a contribution from iNOS. SHHF rats showed significant lipid peroxidation compared with age-matched WKY rats, which was confirmed by EPR spectroscopy and in vivo

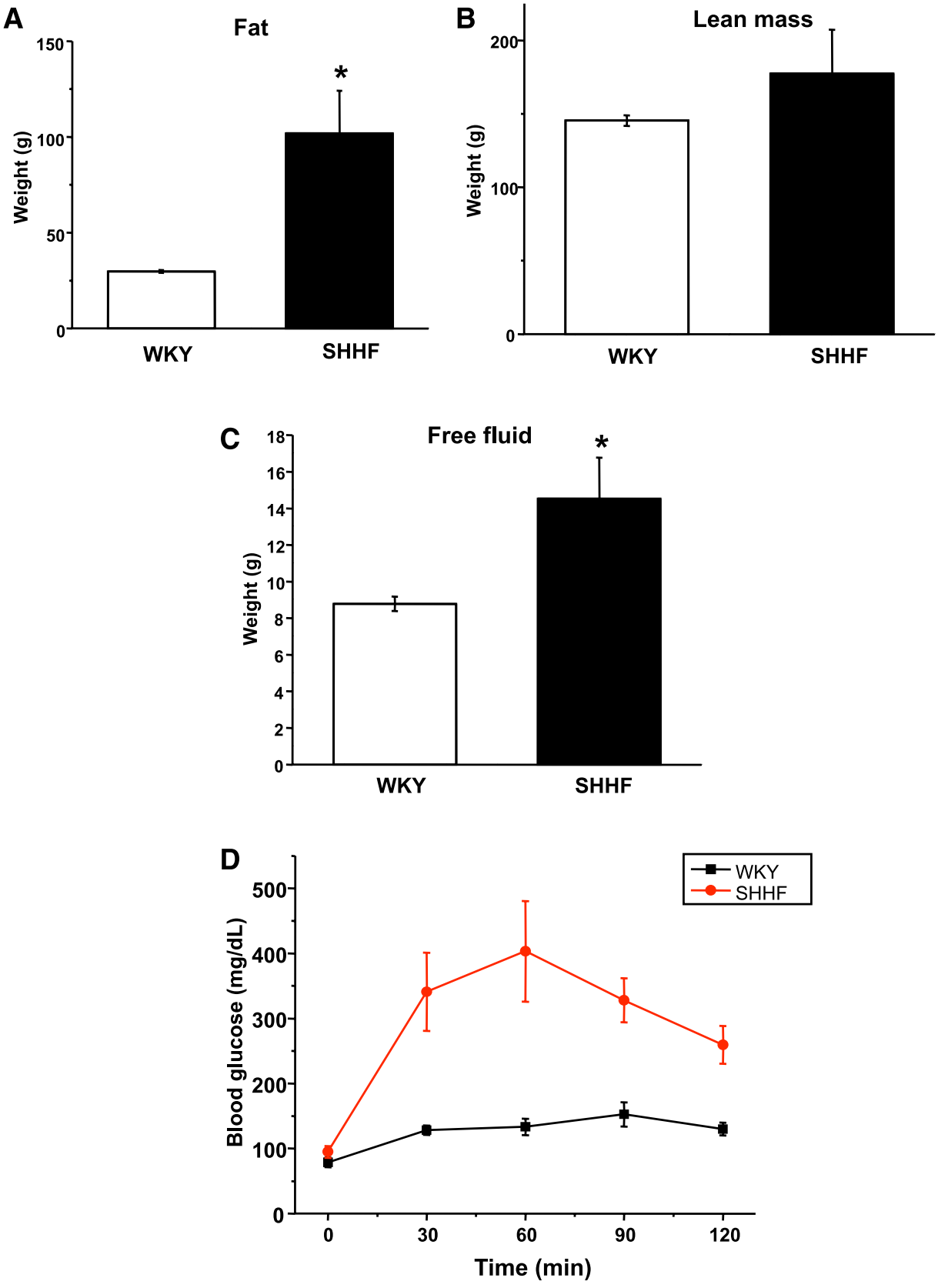

FIG. 1. Body composition and glucose levels after an OGTT in WKY and SHHF rats. SH obese rats showed significantly increased fat (*A*) and free fluid mass (*C*). *B*: Lean mass amount was unchanged. *D*: OGTT showed impaired response in SHHF rats. $n = 6$, $^*P < 0.05$ vs. control. (A high-quality color representation of this figure is available in the online issue.)

spin trapping experiments. These experiments led to the detection of strong six-line EPR signals of a POBN radical adduct that were reproducibly observed in the bile of SHHF rats 2 h after spin trap administration (Fig. 2*A–B*). In WKY, only residual signals of POBN radical adducts were recorded, confirming increased free radical formation in the obese animals. EPR is the unambiguous way to detect radical species; because of their paramagnetic nature, they will give rise to a specific signal. As a result of the radical species' short half-life, it is usually necessary to use spin traps to trap these radicals as adducts with a longer half-life. POBN is specific for carbon-centered radicals, and the whole six-line of the trace indicates a lipid-derived radical species. This is verified from previous simulations using an EPR database. On the basis of the distances between the peaks (hyperfine splitting constants), the detected species is identified unequivocally. The free radicals trapped were identified through their EPR parameters, $a^{N} = 15.75 \pm 0.06$ G and $a_{\beta}^{H} = 2.77 \pm 0.07$ G, corresponding to those reported previously for the POBN radical adduct of a carbon-centered, lipid-derived radical (34) (see also Supplementary Fig. 1).

A significant decrease in the formation of lipid free radical adducts was found in SHHF rats when rats were injected with 1400 W (15 mg/kg i.p.), a specific inhibitor of iNOS (35), 1 h before spin trap administration (Fig. 2*A–B*). The inhibitory effect remained for >2 h. Western blot studies also confirmed elevated iNOS protein levels in the liver of SHHF rats (Fig. 2*C–D*). We were not able to detect iNOS protein in the skeletal muscle. These

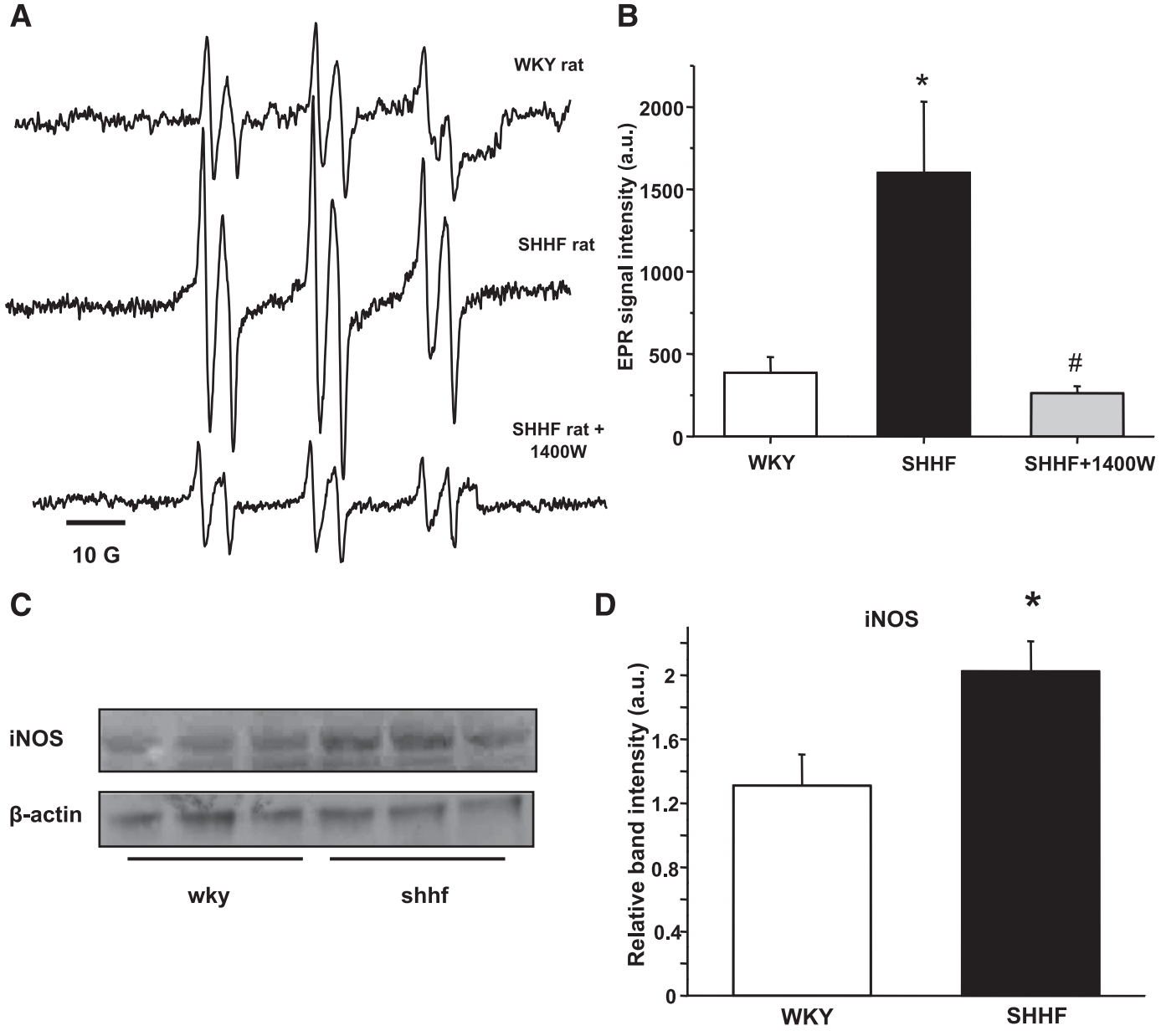

FIG. 2. Lipid free radical generation is increased in the obese SHHF rat as detected by in vivo spin trapping and can be modulated by iNOS inhibition. *A*: Representative spectra of POBN lipid radical adducts in WKY, SHHF, or 1400 W–treated SHHF obese group. Inhibition of iNOS with 1400 W significantly decreased the EPR-detectable lipid radical products in SHHF rats. *B*: Statistical evaluation of the spectra. *C* and *D*: Increased iNOS protein levels in SHHF rat liver homogenates ($n = 6$). *$P < 0.05$ vs. control, #$P < 0.05$ vs. SHHF group. a.u., arbitrary unit.

results suggest a contribution of hepatic iNOS to the radical generation process in these obese rats. Although a specific mechanism is hard, if not impossible, to prove in vivo, this may imply peroxynitrite and its decomposition or reaction with CO_2 in the tissues leading to radical intermediates.

Accumulation of 4-HNE, nitrotyrosine, and nitrite in the liver of SHHF rats. Because SHHF rats showed increased lipid radical production (Fig. 2), which was attenuated by specific iNOS inhibition, we investigated whether iNOS levels and the accumulation of lipid peroxidation or protein oxidation end products, such as 4-HNE and nitrotyrosine, are elevated in liver and skeletal muscle tissues. It is interesting that these two tissues showed different characteristics. Confocal studies colocalized significant 4-HNE and nitrotyrosine accumulation in the liver of obese SHHF rats, but only slight changes were notable in the skeletal muscle, compared with age-matched WKY rats (Fig. 3*A–B*). Consistent with iNOS and nitrotyrosine levels, liver nitrite levels were significantly higher in the obese SHHF liver but only slightly changed in skeletal muscle (Fig. 3*C*). Since iNOS levels were elevated in the liver but not in skeletal muscle, this result suggests that hepatic iNOS overexpression may drive the reactions leading to the accumulation of 4-HNE, 3-nitrotyrosine, and nitrite in the liver, but this process is absent in skeletal muscle.

Impaired insulin signaling cascade in the liver and skeletal muscle of SHHF rats. To gain a better understanding about the possible perturbations of insulin signaling in SHHF rats, we first examined the basal levels of IRS-1 protein and the transcriptional regulators of gluconeogenesis, PGC1-α, PEPCK, and G6Pase. To determine the degree of change in the insulin signaling cascade, IR-β, IRS-1, and Akt proteins were immunoprecipitated from WKY and SHHF rat liver and skeletal muscle tissues after insulin injection. We investigated Tyr phosphorylation on IR-β, the attachment of the p85 subunit of the PI3K protein to IRS-1, and Ser473 phosphorylation on Akt from these samples. SHHF rats did not show decreased levels of IRS-1 in the liver or skeletal muscle; however, expression of the gluconeogenetic master regulators were elevated in the liver, which is typical of many diabetic animal models (Fig. 4*A–B*). Tyr phosphorylation of IR-β was significantly reduced in SHHF rat liver and skeletal muscle, together with impaired p85 attachment to IRS-1 (Fig. 5*A–D*). Akt levels were unchanged, but Ser473 Akt phosphorylation was reduced in both tissues (Fig. 5*E–F*).

Rosiglitazone treatment inhibits lipid radical formation and iNOS expression while enhancing OGTT response and insulin signaling. As the commonly used diabetes drug rosiglitazone has also been suggested to affect iNOS levels, we asked whether rosiglitazone treatment is able to reduce iNOS levels and lipid radical formation in obese rats, while in parallel improving their condition. Ten days of intraperitoneal rosiglitazone treatment significantly reduced the detectable lipid radical formation in the bile and almost completely attenuated the increased iNOS protein levels in the liver (Fig. 6*A–C*).

The treatment also improved OGTT response and corrected the insulin signaling pathway as shown by enhanced phosphorylation and p85 attachment in the liver (Fig. 6*D–E*). Of interest, a 10-day treatment with a general scavenger TEMPOL (30 mg/kg/day) resulted only in a mild improvement of OGTT response (Supplementary Fig. 2), indicating that thiazolidinedione is necessary to achieve both the redox and the insulin-sensitizing effects.

DISCUSSION

Increasing evidence indicates that during the development of insulin resistance, toxic lipid metabolites accumulate in tissues, contributing to the overall reduction of insulin sensitivity (26,36). The possible underlying mechanisms are currently under investigation, but incomplete fatty acid oxidation and the accumulation of lipotoxic metabolites compromise insulin signaling. Here, we studied a lipid peroxidation mechanism and impairment of the insulin signaling cascade of an obese, heart-failure prone, insulin-resistant animal model. We asked whether toxic lipid metabolites accumulate in insulin-sensitive tissues, whether iNOS is a contributing source, and whether thiazolidinedione treatment is able to attenuate lipid radical formation.

The unique methodology of EPR spectroscopy combined with spin trapping allowed us to characterize a lipid radical–driven process in the liver of SHHF rats. We provide in vivo evidence that a lipid radical–generating mechanism contributes to toxic lipid end product accumulation. In spin trapping, short-lived free radical intermediates react with the spin trapping agent, producing stable free radical adducts that are mainly excreted in the bile. These can then be detected and characterized through their unique signature EPR spectra (37). Lipid radical formation was increased in the SHHF rat and was significantly reduced with a specific iNOS inhibitor (1400 W), therefore suggesting the active participation of iNOS in the initial free radical–generating process. POBN gets distributed through the tissues, and POBN radical adducts are excreted in the bile. Although this is a convenient way to detect lipid peroxidation, the method probably reflects hepatic processes only. In contrast to our previous results obtained in a type 1 diabetes model (25), the lipid radical formation was unchanged by L-arginine addition (Supplementary Fig. 1). If iNOS is uncoupled, generating both superoxide and NO, the substrate L-arginine should abrogate the process and restore iNOS coupling. Our data indicate that iNOS is in its coupled state in this model. Furthermore, the addition of DMSO did not improve the EPR signals (Supplementary Fig. 1). DMSO specifically reacts with $^{\bullet}OH$ radicals if present, and $^{\bullet}OH$ is then converted into a methyl radical ($^{\bullet}CH_3$) through its diffusion-limited reaction with DMSO ($k = 7 \times 10^9 \cdot \text{mol/L}^{-1} \cdot \text{s}^{-1}$) (38). The $^{\bullet}CH_3$ radicals are then trapped and detected by EPR as POBN radical adducts, resulting in an additional increase of the initial POBN lipid radical adduct signal. Our data suggests the lack of the $^{\bullet}OH$ radical in the process. The initiation of lipid peroxide generation depends on other contributing mechanisms.

As a result of increased lipid peroxidation, 4-HNE accumulation was also observed in the SHHF liver (Fig. 3*A*). Reactive oxygen species generation stimulates the peroxidation of polyunsaturated fatty acids resulting in lipid hydroperoxide production. Our EPR experiments demonstrated the presence of increased lipid radical formation, which is an intermediate step leading to the generation of primary products of lipid peroxidation, lipid hydroperoxides. Given their unstable nature, the decomposition of these hydroperoxides leads to various reactive aldehydes, including 4-HNE (28). 4-HNE is a well-characterized toxic aldehyde end product of lipid peroxidation that reacts with amine groups to produce covalent modification of proteins and enzymes via nonenzymatic Michael addition (29). We found a strong colocalization of HNE and 3-nitrotyrosine in the liver (Fig. 3*B*), together with increased nitrite formation

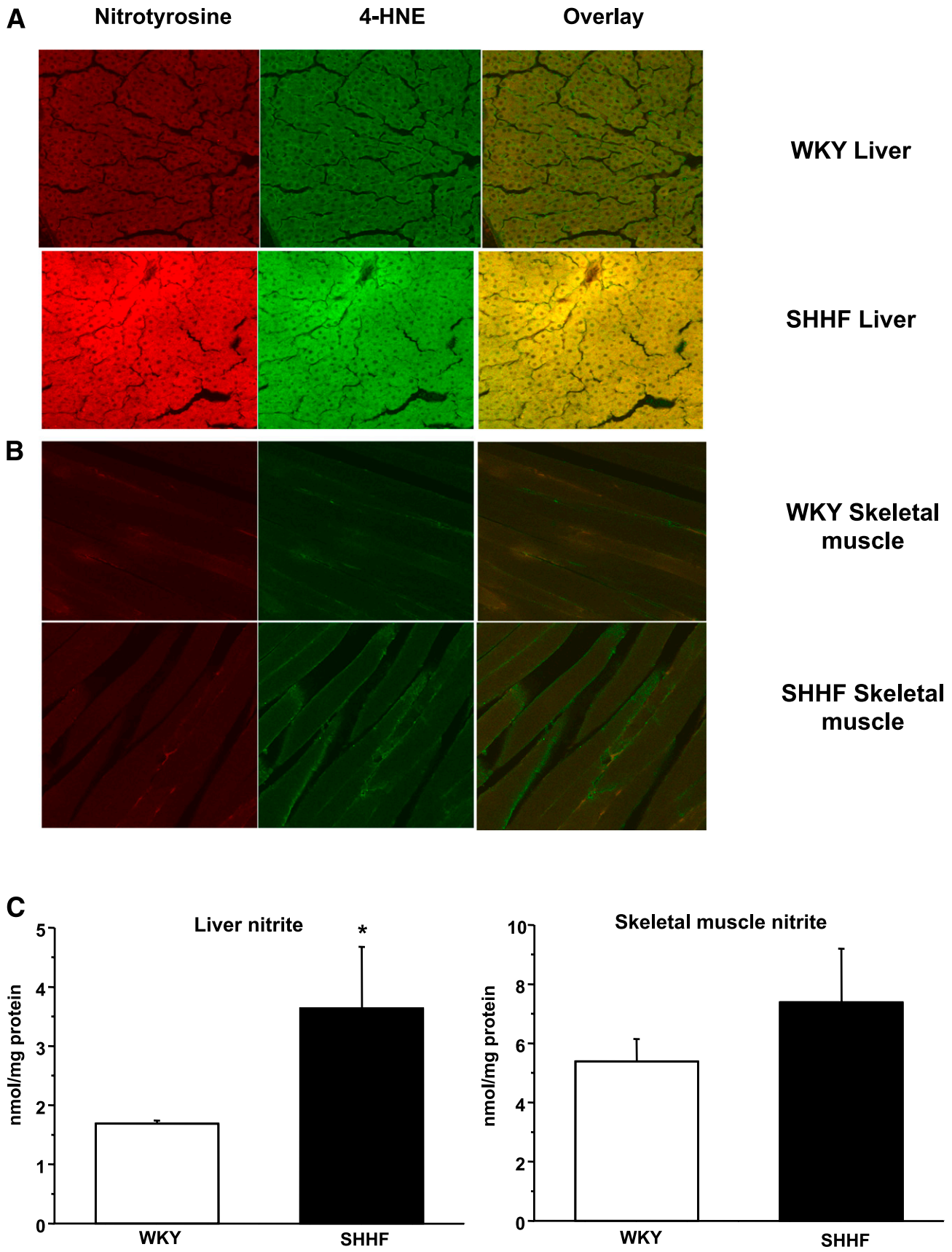

FIG. 3. Detection of 4-HNE, 3-nitrotyrosine, and nitrite in WKY and SHHF rat liver and skeletal muscle tissues. *A*: Red staining shows increased nitrotyrosine levels while green staining indicates elevated 4-HNE levels in the liver of SHHF rats with a great extent of colocalization. *B*: In comparison, only very mild changes were observed in the skeletal muscle. Confocal pictures are representative of six animals per group, three independent slides from each animal. *C*: Liver nitrite levels in SHHF rats showed a significant increase compared with WKY rats, while only slight, not significant changes were observed in skeletal muscle nitrite levels. Tissue samples were collected from three different animals and were run in triplicate on each sample. *$P < 0.05$ vs. control. (A high-quality digital representation of this figure is available in the online issue.)

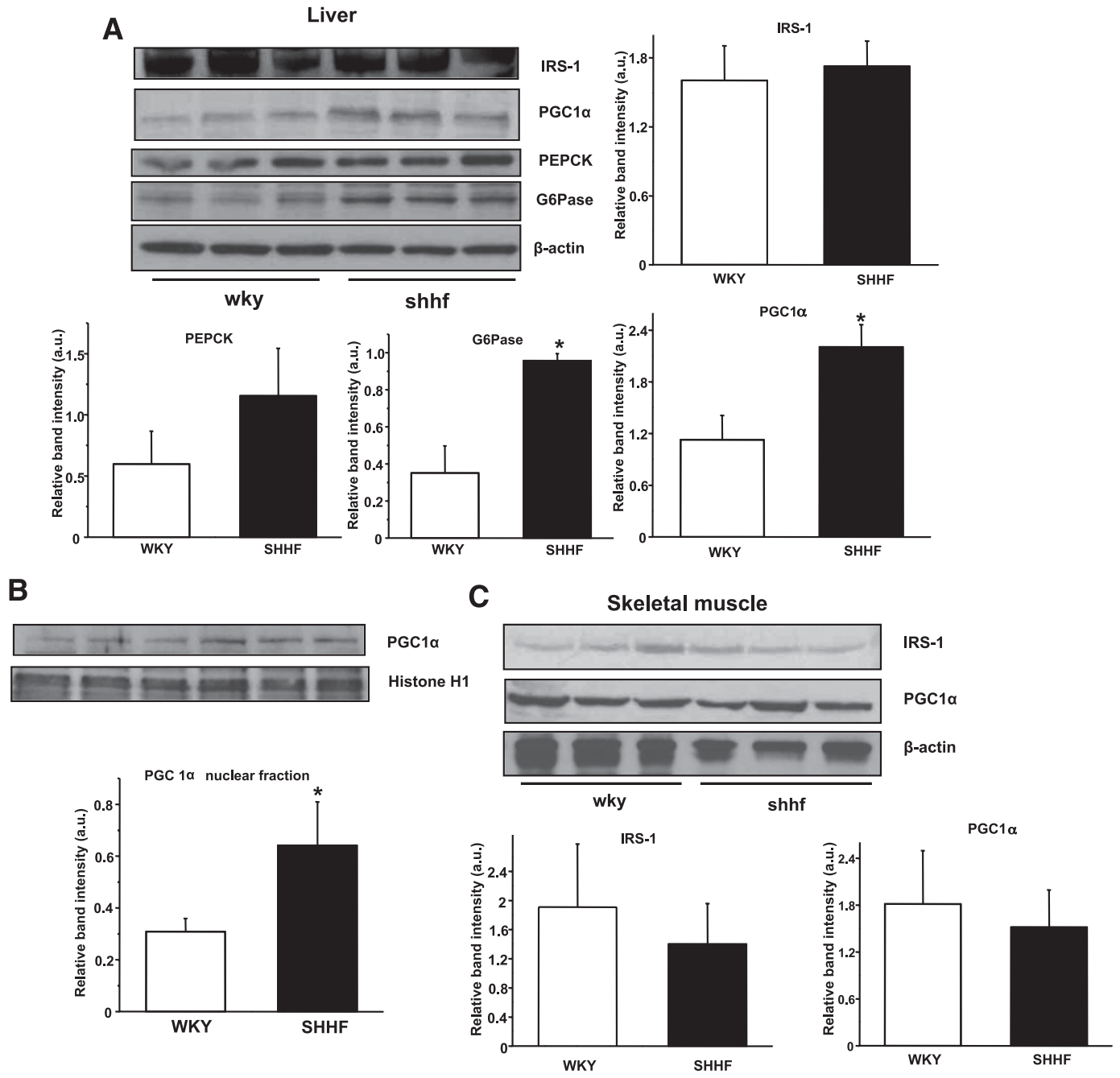

FIG. 4. Effects of obesity on gluconeogenesis and IRS-1 protein levels in insulin-sensitive tissues. *A*: IRS-1 levels were not affected in the liver of SHHF rats, but the levels of the master regulators of hepatic gluconeogenesis (PGC1-α, PEPCK, and G6Pase) were increased. *B*: PGC1-α levels were increased in the hepatic nuclear fraction of SHHF rats. *C*: IRS-1 or PGC1-α levels did not change in the skeletal muscle. $n = 6$, $^*P < 0.05$ vs. control, representative blots of several independent experiments. a.u., arbitrary unit.

(Fig. 3*C*). This observation is particularly interesting because it indicates a correlation of lipid radical production and nitration in vivo and allows a speculation that lipid radical formation can lead to nitration as well through Tyr radical formation. This was recently suggested via in vitro model systems in a hydrophobic environment (32,33).

To further link lipid radical formation and the possible role of proinflammation and iNOS activation, we treated SHHF rats with the diabetes drug rosiglitazone for 10 days. Thiazolidinediones are known to act on not only PPAR-γ but also iNOS and cyclooxygenase; therefore, they may have the potential to inhibit an iNOS-driven lipid radical production. Rosiglitazone treatment not only improved the OGTT response and insulin signaling in obese rats but also led to significantly attenuated lipid radical formation and reduced iNOS protein levels, thus presenting a strong mechanistic link between these oxidative processes (Fig. 6). Here, we show that in addition to the known positive and negative effects, a PPAR-γ agonist can reduce oxidative stress in this model through reducing lipid radical formation possibly with an iNOS-mediated origin. This effect can certainly contribute to a better redox status in insulin-sensitive tissues. Rosiglitazone may have other potential redox effects

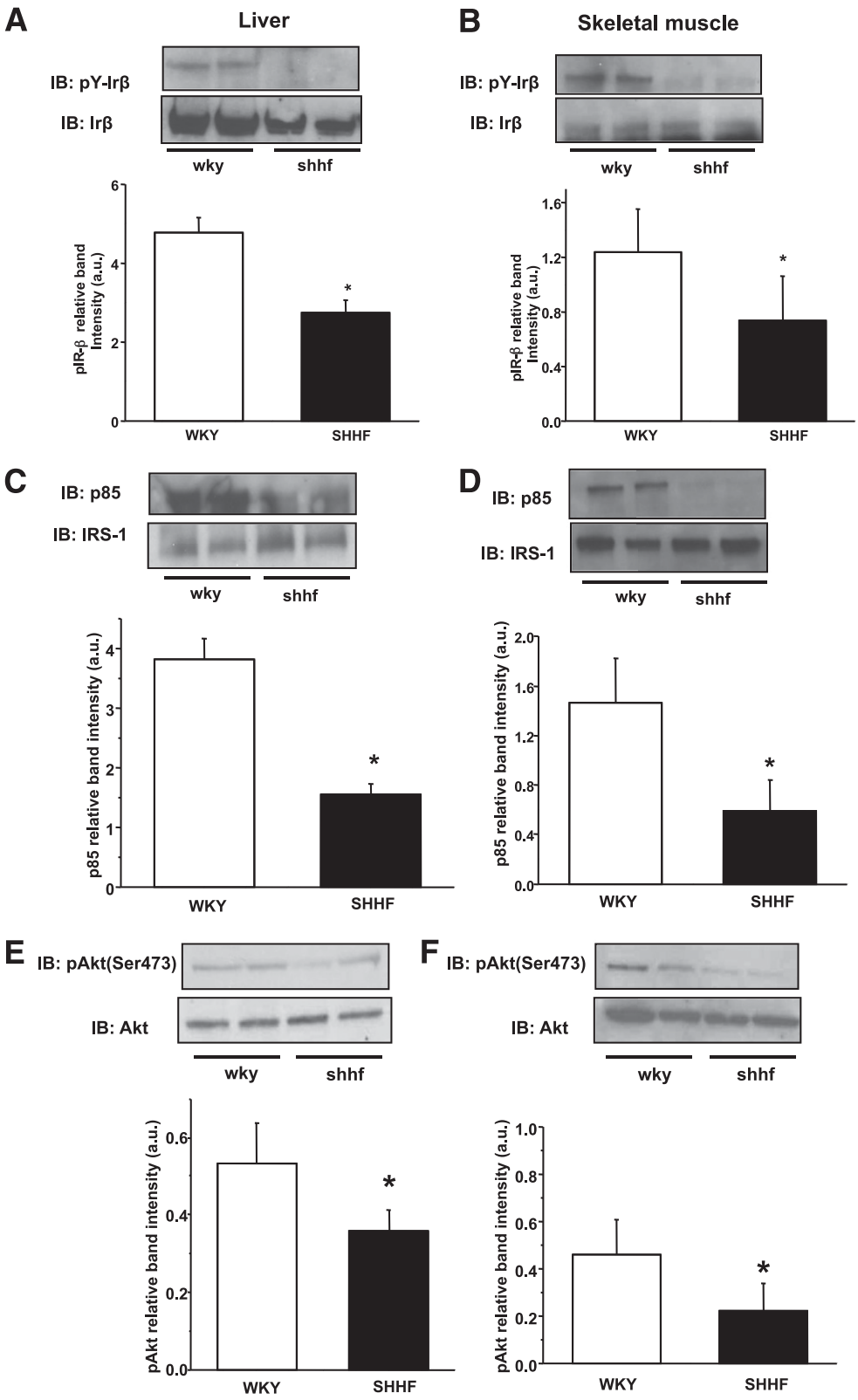

FIG. 5. Characterization of the model-impaired insulin signaling pathway in the liver and skeletal muscle of SHHF rats. *A* and *B*: Impaired Tyr1162/3 phosphorylation of IR-β in both tissues after insulin trigger. *C* and *D*: Significantly less p85-IRS-1 attachment compared with WKY rats in both organs. *E* and *F*: Downstream effect and significantly lower Akt Ser473 phosphorylation in the obese animals in both insulin-sensitive tissues. Bar graphs show the evaluation of the phosphorylation blots relative to their corresponding loading: phospho IR-β relative to IR-β (*A* and *B*), p85 relative to IRS-1 (*C* and *D*), and phospho Akt Ser473 relative to Akt (*E* and *F*). $n = 6$ animals, *$P < 0.05$ vs. control, representative blots and immunoprecipitations of several independent experiments. IB, immunoblotting; a.u., arbitrary unit.

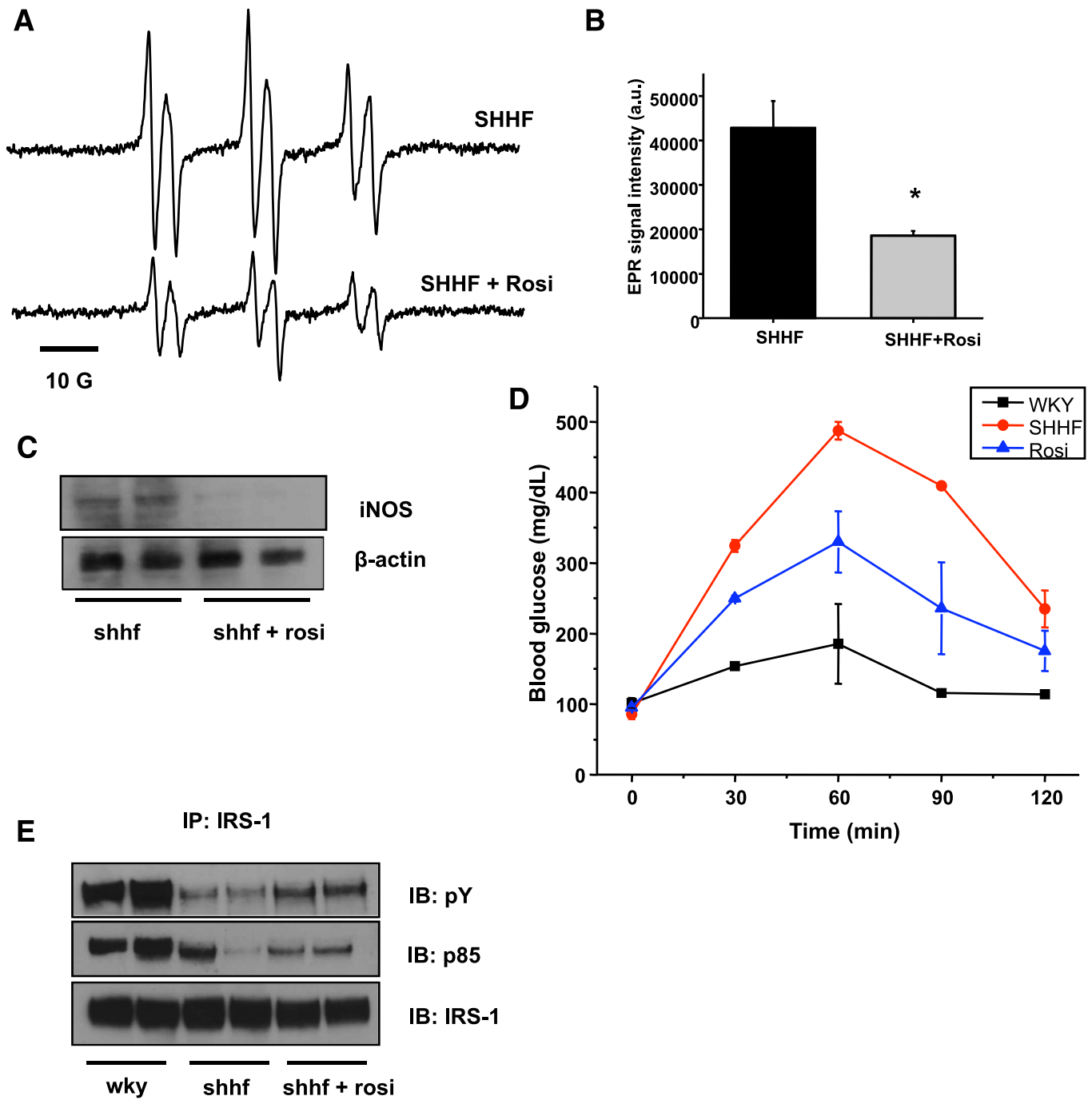

FIG. 6. Rosiglitazone treatment reduces oxidative stress through iNOS modulation while it improves insulin sensitivity in the liver. *A*: Representative spectra of lipid free radical production in SHHF rats before and after a 10-day regimen of rosiglitazone (Rosi) treatment. *B*: Rosiglitazone treatment significantly reduced the level of lipid radical formation ($n = 5$, $^*P < 0.05$). *C*: Treatment almost completely blunted iNOS protein levels in the SHHF rat liver. *D*: Improved OGTT response in SHHF rats after 10 days of thiazolidinedione treatment. *E*: Improved insulin signaling (p85 attachment and IRS-1 phosphorylation) in SHHF liver upon rosiglitazone treatment. $n = 4$, representative blots and immunoprecipitations of several independent experiments. a.u., arbitrary unit; IP, immunoprecipitation; IB, immunoblotting. (A high-quality color representation of this figure is available in the online issue.)

that can contribute to the overall mechanism. It has been implied before that rosiglitazone has anti-inflammatory potential through blocking iNOS and cyclooxygenase, whereas a PPAR-γ antagonist blunted these effects (39). To test whether the PPAR-γ agonist potential is important in our model, we next treated SHHF rats with the general scavenger TEMPOL (30 mg/kg) for 10 days and performed an OGTT after treatment. TEMPOL had only a mild effect and was not able to reduce blood glucose levels significantly (Supplementary Fig. 2). This result indicates that the PPAR-γ agonist activity of rosiglitazone may be important to modulate iNOS levels and subsequent lipid peroxidation, and it is necessary to achieve both the redox and the insulin-sensitizing effects.

Charbonneau and Marette (40) recently showed that lipid infusion in mice induces nitrotyrosine formation, which damages all the major insulin signaling proteins in the IR-β/IRS/PI3K/Akt cascade. An in vitro model from

Bartesaghi et al. (33) shows that lipid peroxides are mediating Tyr oxidation processes in hydrophobic compartments. Our studies are in agreement with those mentioned above in an in vivo model in SHHF rats and further tie the role of iNOS and the subsequent lipid peroxidation process together. While improving glucose tolerance and signaling, treatment with thiazolidinediones can also attenuate oxidative stress through inhibiting lipid radical formation. The detrimental effect of HNE in SHHF rats may occur via a direct mechanism partially disabling protein function. Another possibility is that, as we indicated before, lipid peroxidation itself can trigger the formation of $Tyr^{\cdot}$, which in turn can lead to nitration on functionally important residues. This warrants further studies of possible modifications on insulin signaling proteins and can provide details about the interference of these metabolites. Besides these mechanisms, others have also shown *S*-nitrosation of insulin signaling proteins (41) in various type 2 diabetes or obesity models.

The lipid peroxidation process was accompanied by impaired insulin signaling in SHHF rat liver and skeletal muscle. Previous studies show similar patterns in the aorta of SH (spontaneously hypertensive) rats (42) and that oxidative stress can be a significant factor in activating signaling cascades and hypertension. Because SHHF rats are insulin resistant and glucose intolerant, but are only slightly hyperglycemic or normoglycemic on fasting, our study shows that indeed, oxidative stress and the accumulation of toxic lipid metabolites in peripheral tissues may play a significant role in the development of metabolic syndrome and insulin resistance.

In conclusion, our findings demonstrate that hepatic iNOS induction contributes to lipid radical formation and, therefore, to redox imbalance and to the accumulation of toxic metabolites in obesity. Rosiglitazone treatment not only promotes improved insulin signaling but also attenuates iNOS-mediated lipid radical formation through the reduction of iNOS protein levels. This effect seems to be connected to its PPAR-γ agonist activity. These interactions could be important factors that may connect proinflammation, oxidative stress, and lipotoxicity together in obesity. Future therapies could focus to act on multiple targets, such as iNOS, peroxynitrite, and lipid peroxides, to improve the pathogenesis of insulin resistance and metabolic syndrome.

ACKNOWLEDGMENTS

This work was supported by grants from the National Institutes of Health (R00-DK-083615 to K.S. and T32-AT004094 to S.W.), the Pennington Foundation, the Louisiana Board of Regents (to K.S.), and the American Heart Association (AHA-09SDG2250933 to M.G.B.).

No potential conflicts of interest relevant to this article were reported.

M.B.K. researched data, contributed to discussion, and wrote the manuscript. M.G.B. and S.W. researched data and contributed to discussion. C.R. and E.C. researched data. K.S. designed the concept, directed the experiments, researched data, contributed to discussion, and wrote the majority of the manuscript. K.S. is the guarantor of this manuscript and, as such, had full access to all the data in the study and takes responsibility for the integrity of the data and the accuracy of the data analysis.

The authors are very grateful to Drs. Andre Marette and Alexandre Charbonneau (both from Laval University, Quebec City, Quebec, Canada) and Dr. Jacqueline Stephens (Louisiana State University, Baton Rouge, LA) for helpful discussions.

REFERENCES

1. Hanley AJ, Williams K, Stern MP, Haffner SM. Homeostasis model assessment of insulin resistance in relation to the incidence of cardiovascular disease: the San Antonio Heart Study. Diabetes Care 2002;25:1177–1184
2. Haffner SM. Epidemiology of insulin resistance and its relation to coronary artery disease. Am J Cardiol 1999;84(1A):11J–14J
3. Osei K. Insulin resistance and systemic hypertension. Am J Cardiol 1999;84 (1A):33J–36J
4. White MF. IRS proteins and the common path to diabetes. Am J Physiol Endocrinol Metab 2002;283:E413–E422
5. Aguirre V, Uchida T, Yenush L, Davis R, White MF. The c-Jun NH(2)-terminal kinase promotes insulin resistance during association with insulin receptor substrate-1 and phosphorylation of Ser(307). J Biol Chem 2000;275: 9047–9054
6. Aguirre V, Werner ED, Giraud J, Lee YH, Shoelson SE, White MF. Phosphorylation of Ser307 in insulin receptor substrate-1 blocks interactions with the insulin receptor and inhibits insulin action. J Biol Chem 2002;277:1531–1537
7. Febbraio MA, Pedersen BK. Muscle-derived interleukin-6: mechanisms for activation and possible biological roles. FASEB J 2002;16:1335–1347
8. Marette A. Molecular mechanisms of inflammation in obesity-linked insulin resistance. Int J Obes Relat Metab Disord 2003;27(Suppl. 3):S46–S48
9. Moller DE. Potential role of TNF-alpha in the pathogenesis of insulin resistance and type 2 diabetes. Trends Endocrinol Metab 2000;11:212–217
10. Evans JL, Goldfine ID, Maddux BA, Grodsky GM. Are oxidative stress-activated signaling pathways mediators of insulin resistance and beta-cell dysfunction? Diabetes 2003;52:1–8
11. Shimabukuro M, Zhou YT, Levi M, Unger RH. Fatty acid-induced beta cell apoptosis: a link between obesity and diabetes. Proc Natl Acad Sci U S A 1998;95:2498–2502
12. Perreault M, Marette A. Targeted disruption of inducible nitric oxide synthase protects against obesity-linked insulin resistance in muscle. Nat Med 2001;7:1138–1143
13. Fujimoto M, Shimizu N, Kunii K, Martyn JA, Ueki K, Kaneki M. A role for iNOS in fasting hyperglycemia and impaired insulin signaling in the liver of obese diabetic mice. Diabetes 2005;54:1340–1348
14. Sugita H, Kaneki M, Tokunaga E, et al. Inducible nitric oxide synthase plays a role in LPS-induced hyperglycemia and insulin resistance. Am J Physiol Endocrinol Metab 2002;282:E386–E394
15. Shimabukuro M, Ohneda M, Lee Y, Unger RH. Role of nitric oxide in obesity-induced beta cell disease. J Clin Invest 1997;100:290–295
16. Sharma K, Danoff TM, DePiero A, Ziyadeh FN. Enhanced expression of inducible nitric oxide synthase in murine macrophages and glomerular mesangial cells by elevated glucose levels: possible mediation via protein kinase C. Biochem Biophys Res Commun 1995;207:80–88
17. Ceriello A, Quagliaro L, D'Amico M, et al. Acute hyperglycemia induces nitrotyrosine formation and apoptosis in perfused heart from rat. Diabetes 2002;51:1076–1082
18. Bédard S, Marcotte B, Marette A. Cytokines modulate glucose transport in skeletal muscle by inducing the expression of inducible nitric oxide synthase. Biochem J 1997;325:487–493
19. Kapur S, Bédard S, Marcotte B, Côté CH, Marette A. Expression of nitric oxide synthase in skeletal muscle: a novel role for nitric oxide as a modulator of insulin action. Diabetes 1997;46:1691–1700
20. Zhou YT, Grayburn P, Karim A, et al. Lipotoxic heart disease in obese rats: implications for human obesity. Proc Natl Acad Sci U S A 2000;97:1784–1789
21. Torres SH, De Sanctis JB, de L Briceño M, Hernández N, Finol HJ. Inflammation and nitric oxide production in skeletal muscle of type 2 diabetic patients. J Endocrinol 2004;181:419–427
22. Szabó C, Zanchi A, Komjáti K, et al. Poly(ADP-Ribose) polymerase is activated in subjects at risk of developing type 2 diabetes and is associated with impaired vascular reactivity. Circulation 2002;106:2680–2686
23. Ceriello A, Mercuri F, Quagliaro L, et al. Detection of nitrotyrosine in the diabetic plasma: evidence of oxidative stress. Diabetologia 2001;44:834–838
24. Tannous M, Rabini RA, Vignini A, et al. Evidence for iNOS-dependent peroxynitrite production in diabetic platelets. Diabetologia 1999;42:539–544
25. Stadler K, Bonini MG, Dallas S, et al. Involvement of inducible nitric oxide synthase in hydroxyl radical-mediated lipid peroxidation in streptozotocin-induced diabetes. Free Radic Biol Med 2008;45:866–874
26. Morrison CD, Huypens P, Stewart LK, Gettys TW. Implications of crosstalk between leptin and insulin signaling during the development of diet-induced obesity. Biochim Biophys Acta 2009;1792:409–416

27. Schneider C, Tallman KA, Porter NA, Brash AR. Two distinct pathways of formation of 4-hydroxynonenal. Mechanisms of nonenzymatic transformation of the 9- and 13-hydroperoxides of linoleic acid to 4-hydroxyalkenals. J Biol Chem 2001;276:20831–20838
28. Grimsrud PA, Xie H, Griffin TJ, Bernlohr DA. Oxidative stress and covalent modification of protein with bioactive aldehydes. J Biol Chem 2008;283: 21837–21841
29. Esterbauer H, Schaur RJ, Zollner H. Chemistry and biochemistry of 4-hydroxynonenal, malonaldehyde and related aldehydes. Free Radic Biol Med 1991;11:81–128
30. Awasthi YC, Sharma R, Cheng JZ, et al. Role of 4-hydroxynonenal in stress-mediated apoptosis signaling. Mol Aspects Med 2003;24:219–230
31. Fazio VM, Rinaldi M, Ciafrè S, Barrera G, Farace MG. Control of neoplastic cell proliferation and differentiation by restoration of 4-hydroxynonenal physiological concentrations. Mol Aspects Med 1993;14:217–228
32. Bartesaghi S, Peluffo G, Zhang H, Joseph J, Kalyanaraman B, Radi R. Tyrosine nitration, dimerization, and hydroxylation by peroxynitrite in membranes as studied by the hydrophobic probe N-t-BOC-l-tyrosine tert-butyl ester. Methods Enzymol 2008;441:217–236
33. Bartesaghi S, Wenzel J, Trujillo M, et al. Lipid peroxyl radicals mediate tyrosine dimerization and nitration in membranes. Chem Res Toxicol 2010; 23:821–835
34. Sato K, Kadiiska MB, Ghio AJ, et al. In vivo lipid-derived free radical formation by NADPH oxidase in acute lung injury induced by lipopolysaccharide: a model for ARDS. FASEB J 2002;16:1713–1720
35. Garvey EP, Oplinger JA, Furfine ES, et al. 1400W is a slow, tight binding, and highly selective inhibitor of inducible nitric-oxide synthase in vitro and in vivo. J Biol Chem 1997;272:4959–4963
36. An J, Muoio DM, Shiota M, et al. Hepatic expression of malonyl-CoA decarboxylase reverses muscle, liver and whole-animal insulin resistance. Nat Med 2004;10:268–274
37. Knecht KT, Mason RP. In vivo spin trapping of xenobiotic free radical metabolites. Arch Biochem Biophys 1993;303:185–194
38. Yue Qian S, Kadiiska MB, Guo Q, Mason RP. A novel protocol to identify and quantify all spin trapped free radicals from in vitro/in vivo interaction of HO(.-) and DMSO: LC/ESR, LC/MS, and dual spin trapping combinations. Free Radic Biol Med 2005;38:125–135
39. Cuzzocrea S, Pisano B, Dugo L, et al. Rosiglitazone, a ligand of the peroxisome proliferator-activated receptor-gamma, reduces acute inflammation. Eur J Pharmacol 2004;483:79–93
40. Charbonneau A, Marette A. Inducible nitric oxide synthase induction underlies lipid-induced hepatic insulin resistance in mice: potential role of tyrosine nitration of insulin signaling proteins. Diabetes 2010;59:861–871
41. Carvalho-Filho MA, Ueno M, Hirabara SM, et al. S-nitrosation of the insulin receptor, insulin receptor substrate 1, and protein kinase B/Akt: a novel mechanism of insulin resistance. Diabetes 2005;54:959–967
42. Sugita M, Sugita H, Kaneki M. Increased insulin receptor substrate 1 serine phosphorylation and stress-activated protein kinase/c-Jun N-terminal kinase activation associated with vascular insulin resistance in spontaneously hypertensive rats. Hypertension 2004;44:484–489